

# The unusual X-ray morphology of NGC 4636 revealed by deep Chandra observations: cavities and shocks created by past AGN outbursts

A. Baldi<sup>\*,†</sup>, W. Forman<sup>\*</sup>, C. Jones<sup>\*</sup>, R. Kraft<sup>\*</sup>, P. Nulsen<sup>\*</sup>, L. David<sup>\*</sup>, S. Giacintucci<sup>\*</sup> and E. Churazov<sup>\*\*</sup>

<sup>\*</sup>*Harvard-Smithsonian Center for Astrophysics, 60 Garden St, Cambridge, MA 02138*

<sup>†</sup>*now at INAF-Osservatorio Astronomico di Bologna, Via Ranzani 1, I-40127 Bologna, Italy*

<sup>\*\*</sup>*Max Planck Institut für Astrophysik, Karl-Schwarzschild-Str. 1, 85741 Garching, Germany*

**Abstract.** We present Chandra ACIS-I and ACIS-S observations ( $\sim 200$  ks in total) of the X-ray luminous elliptical galaxy NGC 4636, located in the outskirts of the Virgo cluster. A soft band (0.5-2 keV) image shows the presence of a bright core in the center surrounded by an extended X-ray corona and two pronounced quasi-symmetric, 8 kpc long, arm-like features. Each of this features defines the rim of an ellipsoidal bubble. An additional bubble-like feature, whose northern rim is located  $\sim 2$  kpc south of the north-eastern arm, is detected as well. We present surface brightness and temperature profiles across the rims of the bubbles, showing that their edges are sharp and characterized by temperature jumps of about 20-25%. Through a comparison of the observed profiles with theoretical shock models, we demonstrate that a scenario where the bubbles were produced by shocks, probably driven by energy deposited off-center by jets, is the most viable explanation to the X-ray morphology observed in the central part of NGC 4636.

**PACS:** 95.85.Nv – 98.52.Lp – 98.54.Cm

## INTRODUCTION

It is well known that active galactic nuclei (AGN) play an important role in the evolution of the hot gas in both individual galaxies and clusters of galaxies [e.g. 1, 2, 3, 4, 5, 6]. The so-called ‘AGN feedback’ can cause re-heating of the central cooling regions of a cluster and balance the cooling due to the X-ray emission [see 6, for a review]. AGN are also effective in shaping the morphology of the hot gas halos around individual galaxies and clusters, e.g. giving rise to cavities and bubbles [7].

While several examples of subsonic bubble inflation due to AGN outbursts in individual galaxies are present in the literature [e.g. NGC 507, M 84; 8, 9], supersonic bubble expansion, giving rise to shocks in the hot X-ray emitting gas, has only been observed in a handful of cases [e.g. M 87, NGC 4552; 5, 10]. Another possible case of supersonic bubble expansion could be that of NGC 4636, the dominant galaxy of a group on the outskirts of the Virgo Cluster [ $10^\circ$  or 2.6 Mpc on the sky to the south of M87, at a distance to NGC 4636 of 15 Mpc; 11].

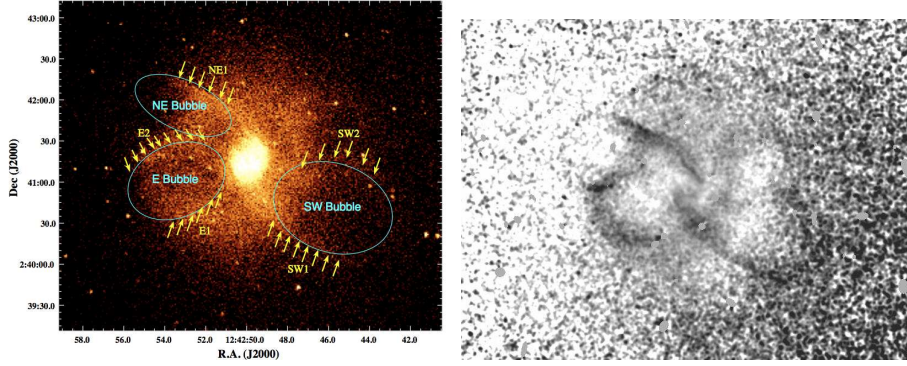


**FIGURE 1.** *Left:* Chandra ACIS-I+ACIS-S image of NGC 4636 in the 0.3-2 keV band. The three bubble-like features detected are labelled and identified by cyan ellipses. The yellow arrows are pointing toward the detected rims of the bubbles. *Right:* Chandra ACIS-I+ACIS-S image after the subtraction of a  $\beta$ -model fitted to the general diffuse X-ray emission.

## CHANDRA DATA PREPARATION AND X-RAY MORPHOLOGY

NGC 4636 was observed twice by ACIS-S and twice by ACIS-I. In our analysis, we use the longer ACIS-S observation (performed on 2000, January 26; ObsID: 323) and both the ACIS-I observations, performed one immediately after the other on 2003, February 14 (ObsID: 3926) and on 2003, February 15 (ObsID: 4415). Details on data preparation and analysis can be found in Baldi et al. [12]. Fig. 1a shows the merged 0.3-2 keV Chandra image of all three observations. The galaxy presents a very bright central core of radius  $\sim 1$  kpc ( $15''$ ) centered on the nucleus. A lower surface brightness region surrounds the nucleus extending out to  $\sim 6$  kpc ( $80''$ ). Two quasi-symmetric arm-like features are embedded in this lower surface brightness emission. These features were previously reported by Jones et al. [13] who analyzed the shorter ACIS-S observation. However, combining these data with the two ACIS-I observations we are able to observe that the south-western arm is clearly part of an X-ray cavity extending as far as  $\sim 9$  kpc ( $2'$ ) from the center. The hint of a similar structure can be observed in coincidence with the north-eastern arm-like feature. It is not clear from the X-ray image whether there is a cavity in this case. The cavities are more evident if we remove the contribution from the general diffuse emission of the galaxy. Fig. 1b shows the merged Chandra image in the 0.3-2 keV band where a  $\beta$ -model fitted to the galaxy diffuse emission was subtracted. This processing allowed to highlight fainter structures.

## THE X-RAY BUBBLES

The most prominent features observed in the Chandra image are the two quasi symmetric 8 kpc long X-ray arm-like structures, already observed by Jones et al. [13] and by O'Sullivan et al. [14]. The SW arm (SW1) is however part of a cavity which extends at least  $\sim 5$  kpc in radius to the North. We performed a spectral analysis in a strip perpendicular to the SW arm-like feature, dividing the strip into rectangles  $\sim 0.5'$  wide, to look for variations in temperature or metal abundance. Although the metallicity does

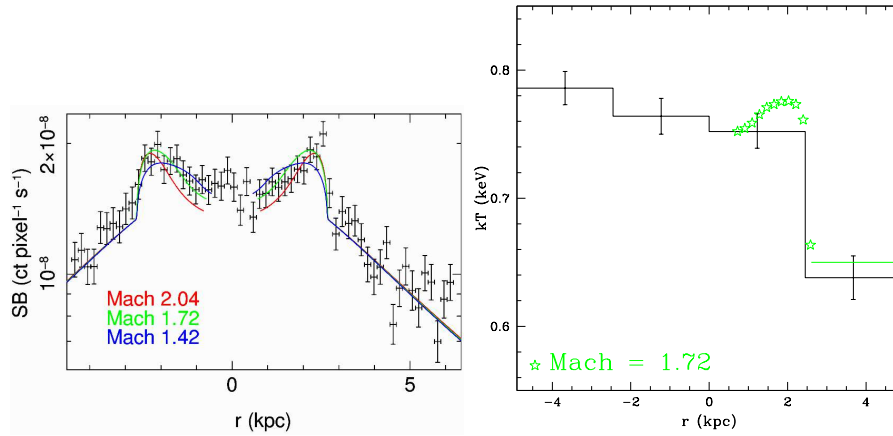


**FIGURE 2.** *Left:* Surface brightness profile perpendicular to the shock front for the SW bubble. The three colored solid lines represents the prediction from a numerical hydro-dynamical shock model at different Mach numbers for the shock. The best fit shock model to the observed data has  $M = 1.72$ . *Right:* Temperature profile across the southern rim of the SW bubble. The temperature jump is consistent with the predictions of a shock model with  $M = 1.72$ .

not vary significantly across the bubble rim, a sharp variation in the temperature was detected coincident with SW1 (Fig. 2) showing a temperature decrease from  $kT \sim 0.75$  keV to  $kT \sim 0.64$  keV, well above the measurement errors ( $\sim 0.01$  keV). A temperature jump was not observed across SW2 most likely because of the complicated geometry of the X-ray emission. Indeed, SW2 seems to be partially embedded in another bubble-like feature located just North of it.

The symmetry of the X-ray arm-like features is highly suggestive of the presence of a symmetric bubble NE of the nucleus of NGC 4636. However the southern rim of the bubble is not clearly visible and it looks instead to be embedded in another round shaped bubble located to the East of the nucleus. If we examine the surface brightness profile of the NE cavity we find a shape which is very similar to the SW bubble. Performing a spectral analysis across the northern cavity rim NE1, we also observe a 20% temperature jump across the rim. However, the scenario in this part of the galaxy is more complex because of the presence of an additional feature just East of the nucleus with the shape of another cavity. This cavity looks less elongated than the other two cavities observed. However, the surface brightness profile has a shape similar to the one across the NE cavity, while the temperature profile shows a temperature jump similar to the one observed in the other two cavities.

### The origin of the cavities: a simple shock model

The most likely scenario for the origin of the cavities observed in the X-ray morphology of NGC 4636 is that they were the result of successive outbursts of the central AGN. In this scenario the jet propagated rapidly from the center, creating a long thin cavity which then inflated in all directions. Perpendicular to the axis of the jet, the ex-

pansion has an approximate cylindrical symmetry. The expanding cavities drive shocks into the surrounding gas.

A 1-dimensional, cylindrically symmetric, time-dependent hydrodynamic model was used to investigate the properties of the shocks for the SW bubble. In this model the sound speed in the relativistic gas that fills the cavity (the piston that drives the shock) is assumed very high, keeping the pressure in the piston nearly uniform. The ratio of the pre-shock pressure to the post-shock pressure determines the strength of the shock. As a result, the shock is weakest (slowest) in the region close to the AGN and fastest in the region farthest from the AGN. Further details on the shock model can be found in Baldi et al. [12].

The calculations of the physical parameters derived from the model were performed for the SW bubble. The three cavities present similar temperature jumps and surface brightness profiles, so similar physical parameters are expected. From the hydrodynamic model, the age of the shock,  $t \sim 2 \times 10^6$  yrs, is the time it takes to expand to its observed size. The age is only sensitive to the shock strength and the temperature of the unshocked gas. This age is slightly shorter than the ratio of the shock radius to the present shock speed, because in the model the shock strength decreases with time (i.e. the shock expanded faster when it was younger). The total energy which produced the shock was  $10^{56}$  ergs, roughly equal to the enthalpy,  $H = 4pV = 7 \times 10^{55}$  ergs, calculated in the assumption that the bubble is predominantly relativistic ( $\gamma = 4/3$ ). The average mechanical power required to produce the bubble equals to  $P_{mech} \sim 1.6 \times 10^{42}$  erg s $^{-1}$ .

## REFERENCES

1. E. Churazov, W. Forman, C. Jones, and H. Böhringer, *A&A* **356**, 788–794 (2000), [arXiv:astro-ph/0002375](#).
2. M. Brüggen, and C. R. Kaiser, *Nature* **418**, 301–303 (2002), [arXiv:astro-ph/0207354](#).
3. A. Cavaliere, A. Lapi, and N. Menci, *ApJL* **581**, L1–L4 (2002), [arXiv:astro-ph/0210431](#).
4. M. Hoeft, and M. Brüggen, *ApJ* **617**, 896–902 (2004), [arXiv:astro-ph/0405434](#).
5. W. Forman, P. Nulsen, S. Heinz, F. Owen, J. Eilek, A. Vikhlinin, M. Markevitch, R. Kraft, E. Churazov, and C. Jones, *ApJ* **635**, 894–906 (2005), [arXiv:astro-ph/0312576](#).
6. B. R. McNamara, and P. E. J. Nulsen, *ARA&A* **45**, 117–175 (2007), 0709.2152.
7. L. Birzan, D. A. Rafferty, B. R. McNamara, M. W. Wise, and P. E. J. Nulsen, *ApJ* **607**, 800–809 (2004), [arXiv:astro-ph/0402348](#).
8. R. P. Kraft, W. R. Forman, E. Churazov, N. Laslo, C. Jones, M. Markevitch, S. S. Murray, and A. Vikhlinin, *ApJ* **601**, 221–227 (2004), [arXiv:astro-ph/0304362](#).
9. A. Finoguenov, M. Ruszkowski, C. Jones, M. Brueggen, A. Vikhlinin, and E. Mandel, *ArXiv e-prints* **807** (2008), 0807.3338.
10. M. Machacek, P. E. J. Nulsen, C. Jones, and W. R. Forman, *ApJ* **648**, 947–955 (2006), [arXiv:astro-ph/0604406](#).
11. J. L. Tonry, A. Dressler, J. P. Blakeslee, E. A. Ajhar, A. B. Fletcher, G. A. Luppino, M. R. Metzger, and C. B. Moore, *ApJ* **546**, 681–693 (2001), [arXiv:astro-ph/0011223](#).
12. A. Baldi, W. Forman, C. Jones, R. Kraft, P. Nulsen, E. Churazov, L. David, and S. Giacintucci, *ArXiv e-prints* (2009), 0904.2569.
13. C. Jones, W. Forman, A. Vikhlinin, M. Markevitch, L. David, A. Warmflash, S. Murray, and P. E. J. Nulsen, *ApJL* **567**, L115–L118 (2002), [arXiv:astro-ph/0108114](#).
14. E. O’Sullivan, J. M. Vrtilek, and J. C. Kempner, *ApJL* **624**, L77–L80 (2005), [arXiv:astro-ph/0503563](#).



